

ORIGINAL RESEARCH

 OPEN ACCESS 

Enhancing anti-tumor efficacy and immune memory by combining 3p-GPC-3 siRNA treatment with PD-1 blockade in hepatocellular carcinoma

Liwei Shao^a, Xin Yu^{a,b}, Qiju Han^a, Xinke Zhang^c, Nan Lu^d, and Cai Zhang ^a

^aInstitute of Immunopharmaceutical Sciences, School of Pharmaceutical Sciences, Cheeloo College of Medicine, Shandong University, Jinan, Shandong, China; ^bCollege of Life Sciences, Ludong University, Yantai, Shandong, China; ^cDepartment of Pharmacology, School of Pharmaceutical Sciences, Cheeloo College of Medicine, Shandong University, Jinan, Shandong, China; ^dInstitute of Diagnostics, School of Medicine, Cheeloo College of Medicine, Shandong University, Jinan, Shandong, China

ABSTRACT

Hepatocellular carcinoma (HCC) is associated with a high mortality rate and presents a major challenge for human health. Activation of multiple oncogenes has been reported to be strongly associated with the progression of HCC. Moreover, the immunosuppressive tumor microenvironment (TME) and the host immune system are also implicated in the development of malignant HCC tumors. Glypican-3 (GPC-3), a proteoglycan involved in the regulation of cell proliferation and apoptosis, is aberrantly expressed in HCC. We synthesized a short 5'-triphosphate (3p) RNA targeting GPC-3, 3p-GPC-3 siRNA, and found that it effectively inhibited subcutaneous HCC growth by raising type I IFN levels in tumor cells and serum and promoting tumor cell apoptosis. Moreover, 3p-GPC-3 siRNA was able to enhance the activation of CD4⁺ T cells, CD8⁺ T cells, and natural killer (NK) cells while reducing the proportion of regulatory T cells (Tregs) in the TME. Most intriguingly, a blocking anti-PD-1 antibody improved the anti-tumor effect of 3p-GPC-3 siRNA, predominantly by activating the immune response, reversing immune exhaustion, and improving immune memory. Our study suggests that the combination of 3p-GPC-3 siRNA administration and PD-1 blockade may represent a promising therapeutic strategy for HCC.

ARTICLE HISTORY

Received 11 July 2021
Revised 21 November 2021
Accepted 22 November 2021

KEYWORDS

Hepatocellular carcinoma; GPC-3; 3p-siRNA; anti-PD-1; immune exhaustion; immune memory; tumor immunotherapy

Introduction

Hepatocellular carcinoma (HCC) is the most common type of primary liver cancer, comprising 75–85% of cases.¹ Treatment options for HCC include surgery, chemotherapy, radiation therapy, and targeted drug therapy. However, overall HCC patient survival remains poor in many countries.² Recently, some immune checkpoint inhibitors have been approved by the Food and Drug Administration (FDA) for the treatment of advanced HCC. Programmed death-1 (PD-1) is a key inhibitory receptor expressed on lymphocytes, with its ligands Programmed death-ligand 1 (PD-L1) and Programmed death-ligand 2 (PD-L2) broadly express on tumor cells.³ The PD-1/PD-L1 interaction elicits inhibitory signals, which exert a wide range of immunosuppressive effects on T cells and NK cells, ultimately leading to their exhaustion.^{4–6} Blocking the PD-1/PD-L1 interaction and the associated signaling pathway can restore the activation and function of exhausted T cells or NK cells.^{4,7} However, the response rates for PD-1/PD-L1 inhibitors are still far from satisfactory.⁸ Therefore, novel therapies for HCC are urgently needed.

The abnormally high expression of proto-oncogenes leads to changes in the biological characteristics of cells, resulting in increased cell proliferation and decreased cell apoptosis. To this end, researchers have designed numerous drugs to target these molecules. Glypicans (GPCs) are a family of heparan sulfate proteoglycans, comprising six subtypes (GPC-1 to

GPC-6), which are linked to the exocyttoplasmic surface of the plasma membrane by a glycosyl-phosphatidylinositol anchor.⁹ GPCs act as co-receptors and control signaling pathways by regulating growth factor/cell-surface receptor interactions.¹⁰ GPC-3 represents a plausible molecular target in HCC due to its abnormally high expression by cancerous cells (which is associated with their lower apoptosis and increased proliferation rates), but absence from normal hepatocytes and benign liver lesions.¹¹ GPC-3 can also potentiate hepatocyte malignancy through the canonical Wnt/ β -Catenin pathway, and its expression positively correlates with poor HCC prognosis and a short overall survival time.¹²

In recent years, the application of RNA interference (RNAi) technology has provided a way to inhibit gene expression and replication *in vitro* and *in vivo*.¹³ In addition, it has been reported that short interfering RNAs (siRNAs) may trigger innate immunity through “off-target” immunostimulatory effects by binding and activating Toll-like receptors (TLRs; e.g., TLR3, 7, and 8), retinoic acid inducible gene I (RIG-I), or protein kinase RNA (PKR).¹⁴ RIG-I is a key sensor of RNA in the cytoplasm of cells; it recognizes RNA with a 5'-triphosphate group (5'-3p siRNA) in a sequence-independent manner.¹⁵ It has been reported that as RIG-I agonists, 3p-siRNAs, can induce type I IFN production by multiple cell types, which plays an important role in activating the innate immune system.^{16,17}

CONTACT Cai Zhang  caizhangsd@sdu.edu.cn, lanan@sdu.edu.cn  Institute of Immunopharmaceutical Sciences, School of Pharmaceutical Sciences, Cheeloo College of Medicine, Shandong University, Jinan, 250012 Shandong, China.

 Supplemental data for this article can be accessed on the [publisher's website](#)

© 2022 The Author(s). Published with license by Taylor & Francis Group, LLC.

This is an Open Access article distributed under the terms of the Creative Commons Attribution-NonCommercial License (<http://creativecommons.org/licenses/by-nc/4.0/>), which permits unrestricted non-commercial use, distribution, and reproduction in any medium, provided the original work is properly cited.

In this study, we synthesized 3p-GPC-3 siRNA targeting GPC-3 and found that it effectively inhibited the growth to the subcutaneous HCC cell line Hepa1-6 by promoting tumor cell apoptosis and immune system activation. Our findings showed that NK cells and CD8⁺ T cells played a pivotal role in the 3p-GPC-3 siRNA-mediated anti-tumor immune responses against HCC. Furthermore, we observed that NK cells and CD8⁺ T cells expressed high levels of PD-1 in the tumor microenvironment (TME) and that PD-1 blockade was able to improve the therapeutic effect exerted by 3p-GPC-3 siRNA by ultimately promoting immune activation, reversing immune exhaustion, and improving immune memory. These findings suggest that a combination of 3p-GPC-3 siRNA administration and PD-1 blockade may provide a promising approach for the treatment of HCC.

Materials and methods

Mice and cell lines

C57BL/6J mice were purchased from HFK Bioscience (Beijing, China). Mice aged 6–8 weeks were used in experiments and were housed in and maintained under specific pathogen-free (SPF) conditions. The Committee on the Ethics of Animal Experiments of Shandong University approved all the animal studies.

The Hepa1-6 and BNL.CL.2 cell lines were purchased from ATCC (Rockville, USA) and cultured in Dulbecco's Modified Eagle Medium (DMEM) supplemented with 10% fetal bovine serum (FBS) at 37°C in a 5% CO₂ incubator. To construct the pSBbi-luc plasmid, the firefly luciferase fragment was amplified from the pGL6-TA plasmid (Beyotime Biotechnology, China) by PCR, prior to being inserted into the pSBbi-GP plasmid (Addgene, USA) via the SfiI restriction site. Hepa1-6 cells were seeded in 6-well plates overnight, then transfected with 1 µg pSBbi-luc plasmid and 1 µg Sleeping beauty SB100X transposase (BioVector NTCC Inc., China) using the *in vitro*-jet PRIME transfection reagent (Polyplus Transfection Inc., USA) according to the manufacturer's instructions. After 24 hours, puromycin (1 µg/mL) was added to screen for stable transfection. The Hepa1-6 cells transfected with these plasmids were named Hepa1-6-GFP-luc⁺ cells.

siRNA synthesis and transfection

DNA templates were purchased from RiboBio Company (Guangzhou, China). A detailed list of all DNA templates is provided in Supplementary Table S1. *In vitro* transcribed siRNAs were synthesized using the *In Vitro* Transcription T7 Kit (Takara, Japan). A list of all siRNA sequences is provided in Supplementary Table S2.

Hepa1-6 cells were transfected with the relevant vector using the *in vitro*-jet PRIME transfection reagent (Polyplus Transfection Inc., USA) according to the manufacturer's instructions. After 48 or 72 hours, the RNA or protein was extracted for subsequent experiments, respectively. DNA-oligonucleotide templates and chemically synthesized siRNA sequences are provided in Supplementary Table S1 and Table S2.

Animal model

1×10^7 Hepa1-6 cells or 1×10^7 Hepa1-6-GFP-luc⁺ cells were injected subcutaneously into the right flank of C57BL/6J mice. When tumors became palpable, mice were randomized into groups, which were intratumorally injected with either 1× phosphate-buffered saline (PBS), 20 µg scramble siRNA, 3p-scramble siRNA, GPC-3 siRNA, or 3p-GPC-3 siRNA, together with the *in vivo*-jet PEI transfection reagent (Polyplus Transfection Inc., New York, USA) every 3 days for a total of four doses. An anti-PD-1 antibody and a rat IgG2a isotype-matched control (RMP1-14, Bio X Cell, USA) were given intraperitoneally at a dose of 200 µg per mouse every 4 days for a total for four doses.¹⁸ The tumor growth was observed continuously and tumor volume was calculated using the formula: $0.5 \times \text{length} \times \text{width}^2$. The tumors were measured using bioluminescence imaging before the mice were sacrificed. Mice were injected intraperitoneally with D-fluorescein (Thermo Fisher Scientific, USA) at a dose of 150 mg per kg of body weight, 10 minutes before imaging. Mice were placed into an IVIS imaging chamber (IVIS Kinetic, Perkin Elmer, USA) after being fully anesthetized using isoflurane (Keyuan Pharmaceutical Co. Ltd, China). The total flux was calculated using Living Image 4.0 software (IVIS Kinetic, Perkin Elmer, USA). The mice were subsequently sacrificed and their tumor weights were measured. Furthermore, the overall survival time of mice was observed, and mice were euthanized when tumors grew to larger than 1,500 mm³.

Reverse transcription-PCR and semiquantitative real-time PCR analysis (qRT-PCR)

Total cellular RNA was extracted with TRIzol (Invitrogen, USA) according to the manufacturer's protocol. Reverse transcription-PCR was performed using M-MLV reverse transcriptase (Invitrogen, USA). For real-time PCR analysis (RT-PCR), cDNA was amplified using the SYBR Green kit (Roche, USA) on an iCycler iQ Real-Time PCR System (Bio-Rad, USA) under standard conditions. Gene expression was normalized to β -actin. A list of PCR primers is provided in Supplementary Table S3.

Western blotting

Cells were collected and lysed on ice using a total protein extraction reagent (Beyotime Biotechnology, China). The protein samples were separated by sodium dodecyl sulfate polyacrylamide gel electrophoresis (SDS-PAGE) and transferred to a nitrocellulose membrane (Millipore, USA). The membrane was blocked in Tris-buffered saline with 5% (w/v) skimmed powdered milk, then incubated with primary antibodies overnight at 4°C, followed by an incubation with a horseradish peroxidase-conjugated secondary antibody for 1 hour at room temperature. Immunoreactive proteins were visualized using the Chemi Doc XRS Imaging System with an XRS camera (Bio-Rad, USA). Rabbit anti-mouse Bcl-2, Bax, Bcl-XL, and Caspase-3 antibodies were purchased from Cell Signaling Technology (New England BioLabs Inc. USA). Rabbit anti-mouse GPC-3 antibody was purchased from Affinity Biosciences (Changzhou, China).

Enzyme-linked immunosorbent assay

Levels of the cytokines IFN- α (ExCell Biology, China) and IFN- β (CUSABIO, China) in the culture supernatant of Hepa1-6 cells and in the serum of tumor-bearing mice were detected by Enzyme-linked immunosorbent assay (ELISA). Concentrations of the cytokines TGF- β , and IL-10 (Multi Sciences Biotech, China) in the serum or tumor tissue homogenate of tumor-bearing mice were also detected by ELISA. ELISAs for cytokine detection were performed according to the manufacturer's instructions.

Measurement of apoptosis

Staining for Annexin V-FITC/PI (Sungene Biotech, China) was used to determine the extent of Hepa1-6 cell apoptosis by flow cytometry (FACS). Total apoptotic cells were subdivided into Annexin V⁺ PI⁻ cells (early apoptosis) and Annexin V⁺ PI⁺ cells (late apoptosis). Alternatively, the apoptosis of tumor tissue was measured by TUNEL staining using a One Step TUNEL Apoptosis Assay Kit (Beyotime Biotechnology, China). Nuclear staining was evaluated under a light microscope using the DAPI reagent (Beyotime Biotechnology, China).

Lymphocyte extraction

The spleens and tumors of the mice were harvested in Roswell Park Memorial Institute (RPMI) 1640 medium supplemented with 10% FBS. Splenocytes were filtered through a 75- μ m cell strainer (Corning, USA) prior to centrifugation. The pelleted cells were then treated with red blood cell lysis buffer (Solarbio Life Science, China) at 4°C for 15 min and 1 \times PBS was added to stop the lysis. Finally, the cells were centrifuged again to obtain a single-cell suspension.

The tumor tissues were cut into small pieces, harvested in RPMI medium supplemented with 2% FBS, 1 mg/mL collagenase IV (Solarbio Life Science, China), 0.1 mg/mL hyaluronidase (Solarbio Life Science, China), and 0.1 mg/mL deoxyribonuclease type I (Roche, USA), and incubated at 37°C for 50 min. The cells were then filtered through a 75- μ m cell strainer and centrifuged. The obtained lymphocyte fraction was further separated from the contaminating tumor cells by centrifugation over a 40% Percoll (Solarbio Life Science, China) gradient at 800 \times g for 25 min at room temperature to obtain a pure fraction of tumor infiltrating lymphocytes (TILs).

Flow cytometry

Tumor infiltrating and splenic lymphocytes were isolated to evaluate the percentages of NK cells, T cells, myeloid-derived suppressor cells (MDSCs), and regulatory T cells (Tregs) as well as the activation status of NK and T cells. The expression of PD-1, CD160, Lag3, CTLA4, TIGIT, and 2B4 on the lymphocytes, the expression of PD-L1 ligands on Hepa1-6 cells and hepatocytes, the percentages of memory T cell subsets (CD3⁺CD8⁺CD44⁺CD62L⁺ or CD3⁺CD8⁺CD44⁺CD62L⁻) and memory T cell subsets expressing CD127 and KLRG1 were also

quantified. Cells were harvested, blocked with an anti-Fc γ R monoclonal antibody (mAb), and stained with anti-mouse fluorochrome-labeled antibodies at 4°C for 45 min. For CD107a and IFN- γ staining, cells were stimulated with phorbol 12-myristate 13-acetate (PMA, 50 ng/mL, Sigma-Aldrich, USA), ionomycin (500 ng/mL, Sigma-Aldrich, USA), monensin (Biolegend, USA), and BFA (Biolegend, USA) for 4 hours, then stained with fluorochrome-labeled anti-mouse antibodies. All stained cells were analyzed on a Gallios flow cytometer (Beckman Coulter, USA), and the data were processed using FlowJo 10 software. A list of the fluorochrome-labeled antibodies used is provided in Supplementary Table S4.

Lymphocyte depletion

For the depletion of NK cells, CD8⁺ T cells, or CD4⁺ T cells, mice were given an intraperitoneal injection of 1 mg anti-NK1.1 mAb (purified from the PK136 hybridoma cell line), 1 mg anti-CD8 mAb (purified from the 2.43 hybridoma cell line),^{19,20} or 500 μ g rat anti-mouse CD4 mAb (clone GK1.5, rIgG2b; Bio X Cell, USA) every 3 days. All cell depletion mAbs were injected into mice 7 days before Hepa1-6 cell challenge. In order to ensure the efficiency of cell depletion, injection of the mAbs was performed during tumor treatment.

Immunofluorescence (IF)

Hepa1-6 cells were cultured on coverslips overnight. Subsequently, the cells were fixed with 4% paraformaldehyde (PFA) for 10 min at room temperature, permeabilized with 0.25% Tween-20 in PBS for 10 min, and then blocked with 5% BSA, 0.3 M glycine in PBS with Tween (PBST) for 1 hour. The cells were incubated with the Ki67 Rabbit mAb (D3B5, Cell Signaling Technology, USA) at 4°C overnight. After three washes with PBST, the cells were incubated with the fluorescently conjugated secondary antibody (DyLight 594, Goat Anti-Rabbit IgG, Abbkine Scientific Co., Ltd, USA) for 1 hour at room temperature. The nuclei were stained with DAPI (Beyotime Biotechnology, China). All images were taken using an inverted fluorescence microscope (IX-71 Inverted microscope, Olympus Company, Japan).

Statistical analysis

Statistical comparisons between two groups were performed using a Student's *t* test. One-way ANOVA was used to compare the differences among more than two groups. Prism 8 (GraphPad) software was used for statistical analysis. All data were shown as the mean \pm standard deviation (SD). *P* values < .05 were considered significant.

Results

3p-GPC-3 siRNA exerts an anti-tumor effect by silencing GPC-3 and stimulating the production of type I IFNs

In our previous study, we successfully synthesized short 5'-triphosphate (3p) RNA, transcribed from a DNA template by T7 RNA polymerase, and found that it could effectively silence

the target molecules and stimulate the production of type I IFNs in a RIG-I-dependent manner.²¹ Here, we initially confirmed the function of 3p-GPC-3 siRNA. The murine HCC cell line Hepa1-6, which expresses high levels of GPC-3, was used here as a cellular model to explore the function of siRNA (**Fig. S1A**). As expected, transfection with GPC-3 siRNA (si-GPC-3) and 3p-GPC-3 siRNA (3p-si-GPC-3) significantly reduced GPC-3 expression in Hepa1-6 cells at both the mRNA and protein level, with no differences observed between the si-GPC-3 and 3p-si-GPC-3 groups (**Fig. S1B-C**). Furthermore, the expression of GPC-3 in Hepa1-6 cells did not diminish after transfection with 3p-scramble siRNA (3p-si-scramble) or scramble siRNA (si-scramble) (**Fig. S1B-C**). We subsequently measured the levels of RIG-I and type I IFNs expressed by Hepa1-6 cells. 3p-si-scramble and 3p-si-GPC-3 transfection significantly increased the expression of RIG-I, IFN- α , and IFN- β mRNA within Hepa1-6 cells (**Fig. S1D-E**). In addition, the levels of IFN- α and IFN- β secreted by Hepa1-6 cells were also elevated (**Fig. S1E**). These results collectively indicate that we had successfully synthesized a 3p-GPC-3 siRNA with both GPC-3-silencing and type I IFNs-eliciting properties.

To explore the anti-tumor effect of 3p-si-GPC-3 *in vivo*, 1×10^7 Hepa1-6 cells were administered subcutaneously to C57BL/6J mice. After the tumor was palpable, the mice were treated with either 1 \times PBS (the control group, CTRL), si-scramble, 3p-si-scramble, si-GPC-3, or 3p-si-GPC-3 via intratumoral multi-point injection every 3 days for a total of four injections. After 14 days, the mice were sacrificed, and the tumor weights were determined. Compared to si-scramble, treatment with 3p-si-scramble, si-GPC-3, or 3p-si-GPC-3 significantly suppressed tumor growth, with the most significant inhibitory effect seen following 3p-si-GPC-3 treatment (**Figure 1a-b**).

Next, we intended to determine whether 3p-si-GPC-3 could play an immunostimulatory role *in vivo*. The levels of cytokines IFN- α and IFN- β in the serum of tumor-bearing mice were determined by ELISA. The results showed that the levels of IFN- α and IFN- β in the serum were significantly higher in the 3p-si-scramble and 3p-si-GPC-3 treatment groups compared to that in the si-scramble (**Figure 1c**). Previous studies had reported that GPC-3 was associated with apoptosis in the context of HCC.²² To this end, we next sought to determine whether 3p-si-GPC-3 could inhibit the proliferation of tumor cells by promoting apoptosis. The results showed that treatment with si-GPC-3 and 3p-si-GPC-3 markedly induced apoptosis in tumor tissues as verified by the fluorescence-based TUNEL assay, while 3p-si-scramble or si-scramble had little pro-apoptotic effect compared to the control group (**Figure 1d**). Collectively, these results suggest that treatment with 3p-si-GPC-3 indeed stimulates the production of type I IFNs and induces apoptosis of tumor cells *in vivo*.

To confirm the role of 3p-si-GPC-3 in HCC, we also performed experiments *in vitro*. The apoptosis of Hepa1-6 cells was detected by Annexin V/PI double staining and FACS analysis. We found that the silencing of GPC-3 (in the si-GPC-3 and 3p-si-GPC-3 groups) significantly promoted the apoptosis of Hepa1-6 cells. Moreover, transfection with 3p-si-scramble had no effect compared to with si-scramble

(**Figure 1e**). We subsequently determined the expression of the apoptosis-related molecules Bcl-2, Bcl-XL, Bax, and Caspase-3 by Western blotting. Silencing of GPC-3 by si-GPC-3 or 3p-si-GPC-3 markedly lowered the protein levels of the anti-apoptotic molecules Bcl-2 and Bcl-XL and increased that of pro-apoptotic molecules Bax and Caspase-3 (**Figure 1f**). These data indicate that silencing of GPC-3 activates the apoptosis-related signal pathway in Hepa1-6 cells. Next, the effect of GPC-3 silencing on cell proliferation was observed by assaying for the proliferation maker Ki67 in Hepa1-6 cells via IF. We observed a marked downregulation of Ki67 in GPC-3-silenced cells (in the si-GPC-3 and 3p-si-GPC-3 groups) as compared to the si-scramble group (**Figure 1g**).

In summary, these results suggest that 3p-GPC-3 siRNA can promote apoptosis and inhibit the proliferation of Hepa1-6 cells by silencing GPC-3, stimulate the production of type I IFN, and ultimately exert an anti-tumor effect *in vivo* and *in vitro*.

3p-GPC-3 siRNA activates NK cells and T cells *in vivo*

The pivotal role of type I IFN in the regulation and activation of innate and adaptive immune responses has been well documented.^{23,24} In order to evaluate whether 3p-si-GPC-3 treatment further stimulated the tumor-suppressive immune responses, we examined the proportions and activation of CD4⁺ T, CD8⁺ T, and NK cells in the tumor tissues and spleens of tumor-bearing mice. According to our FACS analyses, the proportions and activation (CD69⁺) of CD4⁺ T, CD8⁺ T, and NK cells in the tumor tissues were increased significantly in both 3p-si-scramble and 3p-si-GPC-3 treated mice (**Figure 2a-b**). In addition, the proportions of suppressor cells including Tregs and MDSCs were also determined. Within the CD4⁺ T cell subset, Tregs numbers were markedly decreased in the 3p-si-scramble and 3p-si-GPC-3 groups, while the proportions of MDSCs did not change significantly (**Figure 2c**). Treatment with si-GPC-3 had little effect on the immune cell composition of tumor tissues (**Figure 2a-c**). Additionally, the proportions of splenic lymphocytes and their activation status were analyzed in tumor-bearing mice. We found that 3p-si-scramble and 3p-si-GPC-3 strongly enhanced the proportions of CD8⁺ T and NK cells as well as the activation of CD4⁺ T, CD8⁺ T, and NK cells in the spleen (**Fig. S2A-B**). In contrast to our observations at the tumor site, 3p-si-scramble and 3p-si-GPC-3 treatment did not change the percentages of CD4⁺ T cells in the spleen (**Fig. S2A**). In addition, there was no significant change in the proportions of MDSCs and Tregs in the spleens of mice belonging to different treatment groups (**Fig. S2C**).

To further investigate which immune cells were involved in the anti-tumor responses observed, NK cells, CD8⁺ T cells, or CD4⁺ T cells were individually depleted using depletion mAbs.^{19,20} The efficiency of lymphocyte depletion is shown in **Figure S3A**. It is seen that the efficiency was maintained until the mice were sacrificed. When the solid tumors were established, 3p-si-GPC-3 was administered to tumor-bearing mice via intratumoral injection and the growth of tumors was observed. As shown in **Figure 2d**, depletion of NK and CD8⁺

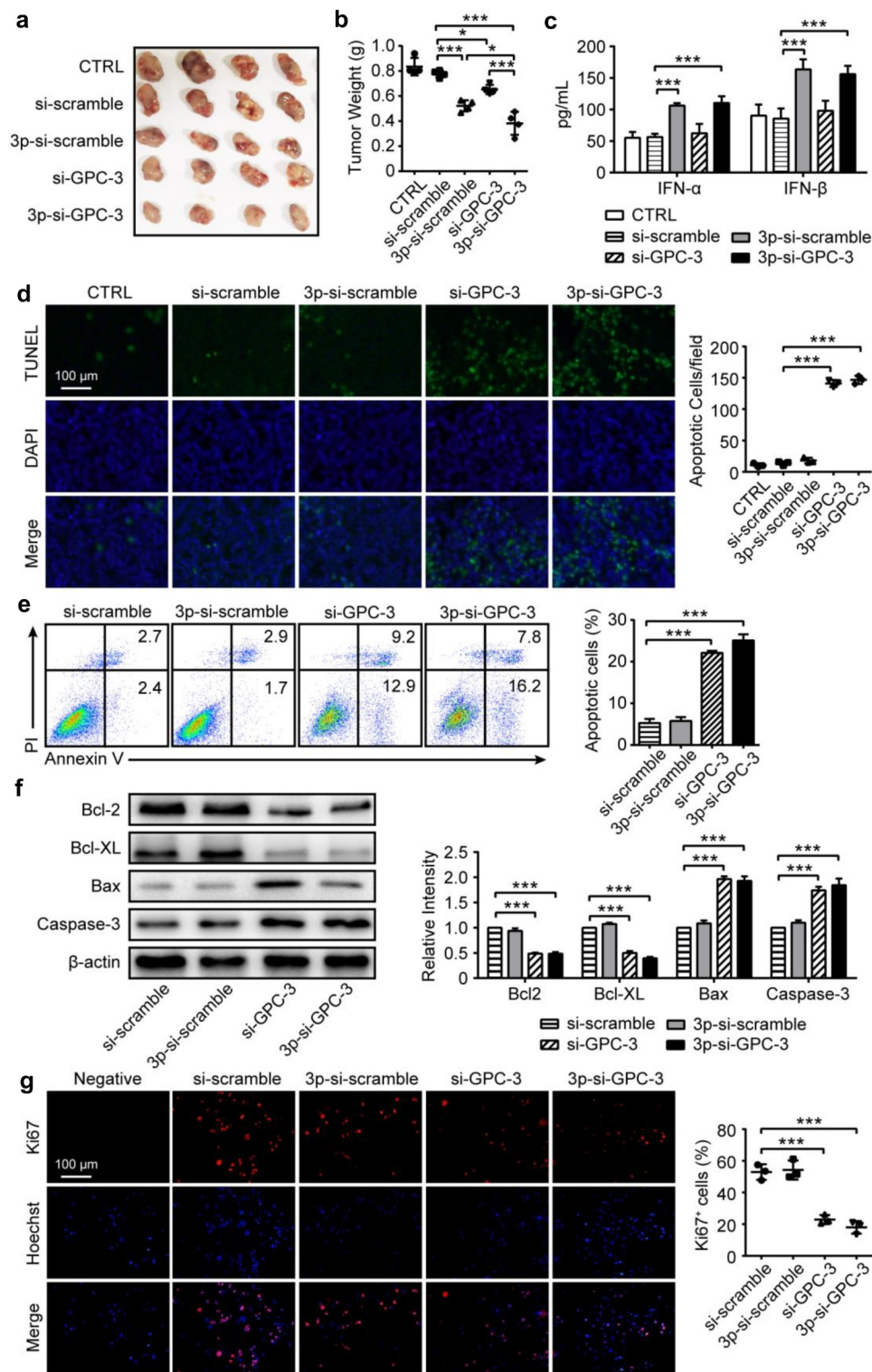


Figure 1. 3p-GPC-3 siRNA inhibits tumor growth by promoting tumor cell apoptosis and the secretion of type I IFNs by immune cells *in vivo* and *in vitro*. (a) C57BL/6J mice were subcutaneously challenged with 1×10^7 Hepa1-6 cells. Si-scramble, 3p-si-scramble, si-GPC-3, or 3p-si-GPC-3 were administered intratumorally every 3 days for a total of four doses, prior to observing tumor growth ($n = 4$). (b) Statistical analysis of tumor weight after treatment with the indicated siRNAs. (c) The serum levels of IFN- α and IFN- β were confirmed by ELISA. (d) (Left) TUNEL (green fluorescence) staining to evaluate apoptosis of HCC tumor cells following various treatment conditions. Nuclei were stained with DAPI (blue fluorescence). (Right) Statistical analysis of TUNEL staining to evaluate the extent of HCC tumor apoptosis. (e) FACS analysis of Hepa1-6 cell apoptosis, using Annexin V/PI double staining, after transfection for 48 hours with the indicated siRNA. (f) Western blotting detection of the protein levels of Bcl-2, Bcl-XL, Bax, and Caspase-3 in Hepa1-6 cells after transfection for 72 hours with the indicated siRNA. (g) IF staining to detect Ki67 expression (red fluorescence) of Hepa1-6 cells after transfection for 72 hours. * $P < .05$, *** $P < .001$.

T cells significantly attenuated 3p-si-GPC-3-induced tumor growth inhibition (Figure 2e), while depletion of CD4⁺ T cells had no effect (Fig. S3B).

Overall, these results indicate that 3p-si-scramble and 3p-si-GPC-3 promote the proliferation and activation of CD4⁺ T, CD8⁺ T, and NK cells at both the systemic and localized tumor

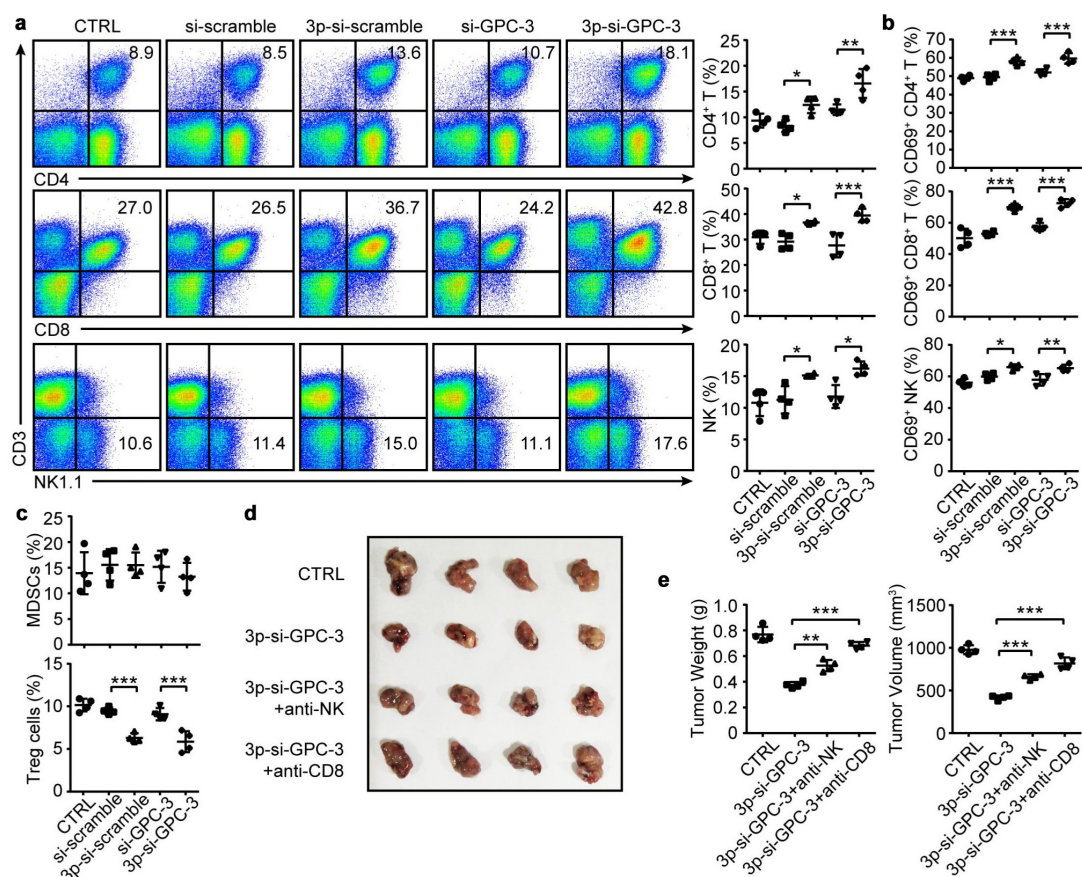


Figure 2. 3p-GPC-3 siRNA activates tumor-infiltrating NK cells and T cells *in vivo*. (a) The percentages of tumor-infiltrating CD4⁺ T cells, CD8⁺ T cells, and NK cells, as determined by flow cytometry. (b) CD69 expression on tumor-infiltrating CD4⁺ T cells, CD8⁺ T cells, and NK cells, as determined by flow cytometry. (c) Flow cytometric quantification of the percentages of tumor-infiltrating MDSCs and Tregs. HCC bearing mice were injected intraperitoneally with depleting antibodies (anti-CD8b and anti-NK1.1) every 3 days until the end of experiment to deplete CD8⁺ T and NK cells. 3p-si-GPC-3 was administered intratumorally every 3 days for a total of four doses, prior to tumor observation. (d) Image showing tumor sizes after treatment (n = 4). (e) Tumor weight and tumor volume were determined. **P* < .05, ***P* < .01, ****P* < .001. *P* > .05 refers to no statistical difference (not shown).

tissue levels, while reducing the number of tumor-infiltrating Tregs, leading to enhanced anti-tumor effects. These data highlight the important role of NK cells and CD8⁺ T cells but not CD4⁺ T cells in the 3p-GPC-3 siRNA-mediated anti-tumor immune responses against HCC.

Anti-PD-1 antibody administration effectively improves the therapeutic effect of 3p-GPC-3 siRNA

It is well established that immune escape via the PD-1/PD-L1 axis plays a key role in HCC development. Accordingly, tumor-infiltrating CD8⁺ T and NK cells have been shown to express high levels of PD-1 in HCC.^{25,26} In our previous study, we found that PD-L1 levels were significantly increased in the central regions of human liver cancer tissues.²⁷ Consequently, we considered whether the immunosuppressive TME would alter the effector functions of CD8⁺ T and NK cells, ultimately limiting the therapeutic impact of 3p-GPC-3 siRNA. Initially, we assessed PD-1 and PD-L1 expression in the TME of the HCC model mice. Our FACS analysis revealed that the expression of PD-L1 was significantly higher in Hepa1-6 cells compared with hepatocytes (Fig. S4A). Furthermore, PD-1 expression was barely detectable on the surface of CD8⁺

T and NK cells derived from the livers of normal mice, but was highly expressed in tumor-infiltrating CD8⁺ T and NK cells (Fig. S4B). This presented us with an opportunity for anti-PD-1 antibody treatment with the aim of improving the therapeutic efficacy of 3p-GPC-3 siRNA.

To this end, mice were given an injection of 1×10^7 Hepa1-6-GFP-luc⁺ tumor cells subcutaneously, followed by treatment with intratumoral 3p-GPC-3 siRNA every 3 days for a total of four doses, together with intraperitoneal PD-1 blocking antibody given every 4 days for a total of four doses (Figure 3a). As shown in Figure 3b-d, compared to the scramble siRNA and IgG group (si-scramble+IgG), monotherapy with anti-PD-1 (si-scramble+αPD-1) or 3p-GPC-3 siRNA (3p-si-GPC-3+IgG) visibly inhibited tumor growth. Meanwhile, 3p-GPC-3 siRNA and anti-PD-1 antibody combination therapy (3p-si-GPC-3+αPD-1) inhibited tumor growth more effectively. Furthermore, we observed the overall survival time of mice. We found that the survival time of mice was effectively prolonged by treatment with 3p-si-GPC-3, anti-PD-1 blocking antibody, and combination therapy. The combination therapy group showed the longest survival time. These results strongly suggest that the anti-tumor effect induced by the 3p-GPC-3 siRNA could be further improved by combination with PD-1 blockade.

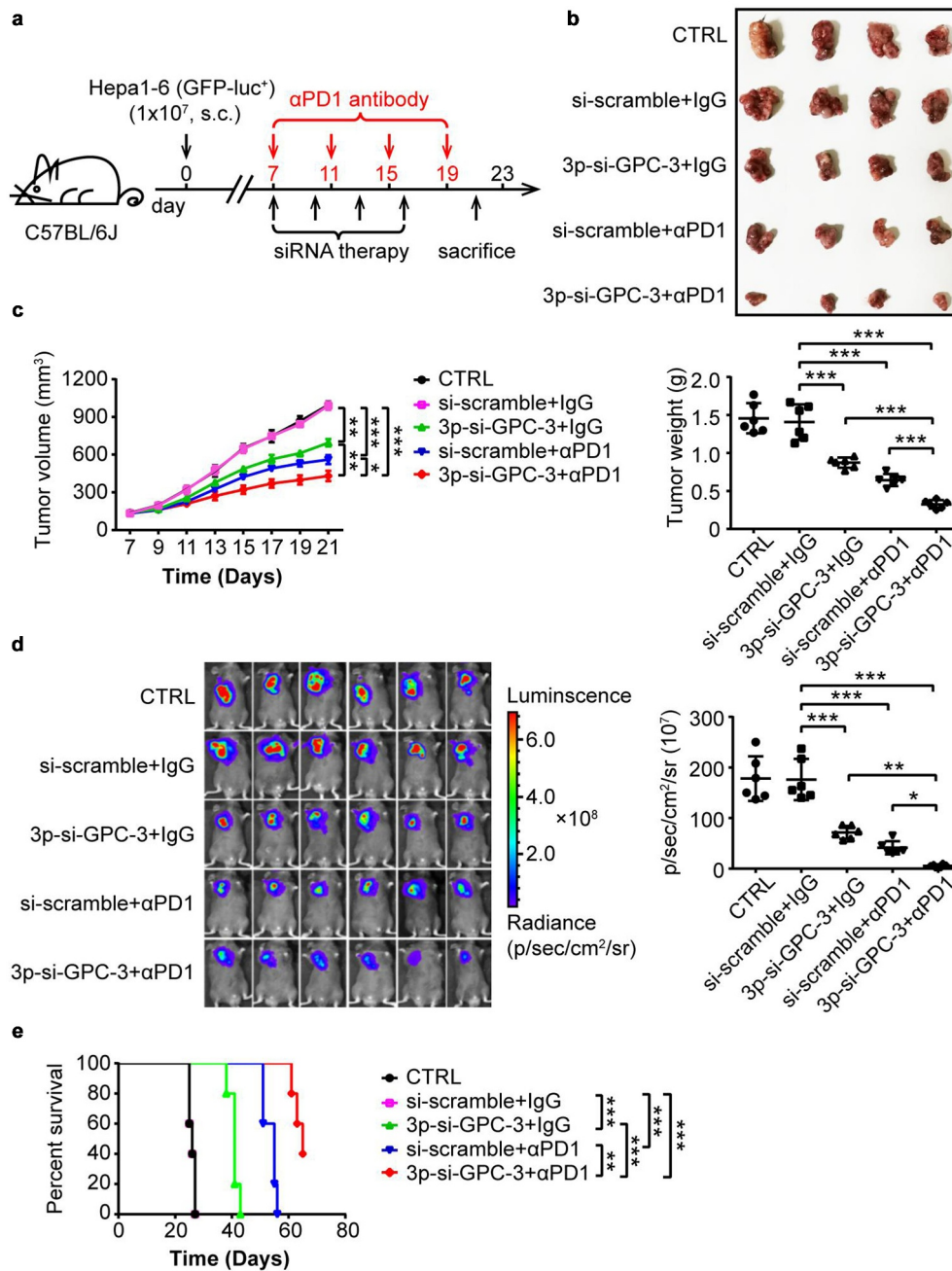


Figure 3. A combination of 3p-GPC-3 siRNA and anti-PD-1 antibody more effectively inhibits tumor growth than 3p-GPC-3 siRNA or anti-PD-1 monotherapy. (a) Treatment schematic. Mice were given an injection of 1×10^7 Hepa1-6-GFP-luc⁺ tumor cells subcutaneously. HCC-bearing mice were injected intraperitoneally with 200 μ g anti-PD1 antibodies every 4 days for a total of four doses, and 3p-GPC-3 siRNA was administered intratumorally every 3 days for a total of four doses. (b) Image showing tumors derived from each treatment group ($n = 4$). (c) Tumor growth curves (left) and tumor weight measurements (right). (d) *In vivo* bioluminescence imaging of subcutaneous tumors in mice ($n = 6$) after treatment as in (a); left, and a quantitative representation of the fluorescence values (right). (e) Survival time of mice bearing Hepa1-6 tumors following treatment with 3p-GPC-3 siRNA, anti-PD1 antibody or combination therapy. Statistical significance was determined by the log-rank test. * $P < .05$, ** $P < .01$ or *** $P < .001$.

PD-1 blockade enhances the anti-tumor effect of 3p-GPC-3 siRNA treatment by improving CD8⁺ T and NK cell function

In order to assess whether the immune system would be further activated in tumor-bearing mice following PD-1 blockade combination therapy, we initially examined the percentages and activation of CD8⁺ T and NK cells in tumor tissues. The proportions of tumor-resident CD8⁺ T and NK cells and their activation status (determined by

their CD69 expression levels) were significantly increased by treatment with 3p-si-GPC-3 or an anti-PD-1 blocking antibody, especially when used in combination (Figure 4a-b). In the spleen, we found that the combination of anti-PD-1 and 3p-si-GPC-3 treatment not only significantly increased the fraction of CD8⁺ T cells but also the CD69 expression on CD8⁺ T and NK cells, compared to treatment with either reagent alone (Fig. S6A-B). Subsequently, the presence of effector markers such as IFN- γ and CD107a was determined

in splenic CD8⁺ T cells and NK cells by flow cytometry. The results showed that every treatment group exhibited elevated CD8⁺ T cell- and NK cell-mediated IFN- γ secretion, and

that these IFN- γ levels were even higher in the combination treatment group when compared to the other groups (Figure 4c). CD107a expression was significantly enhanced

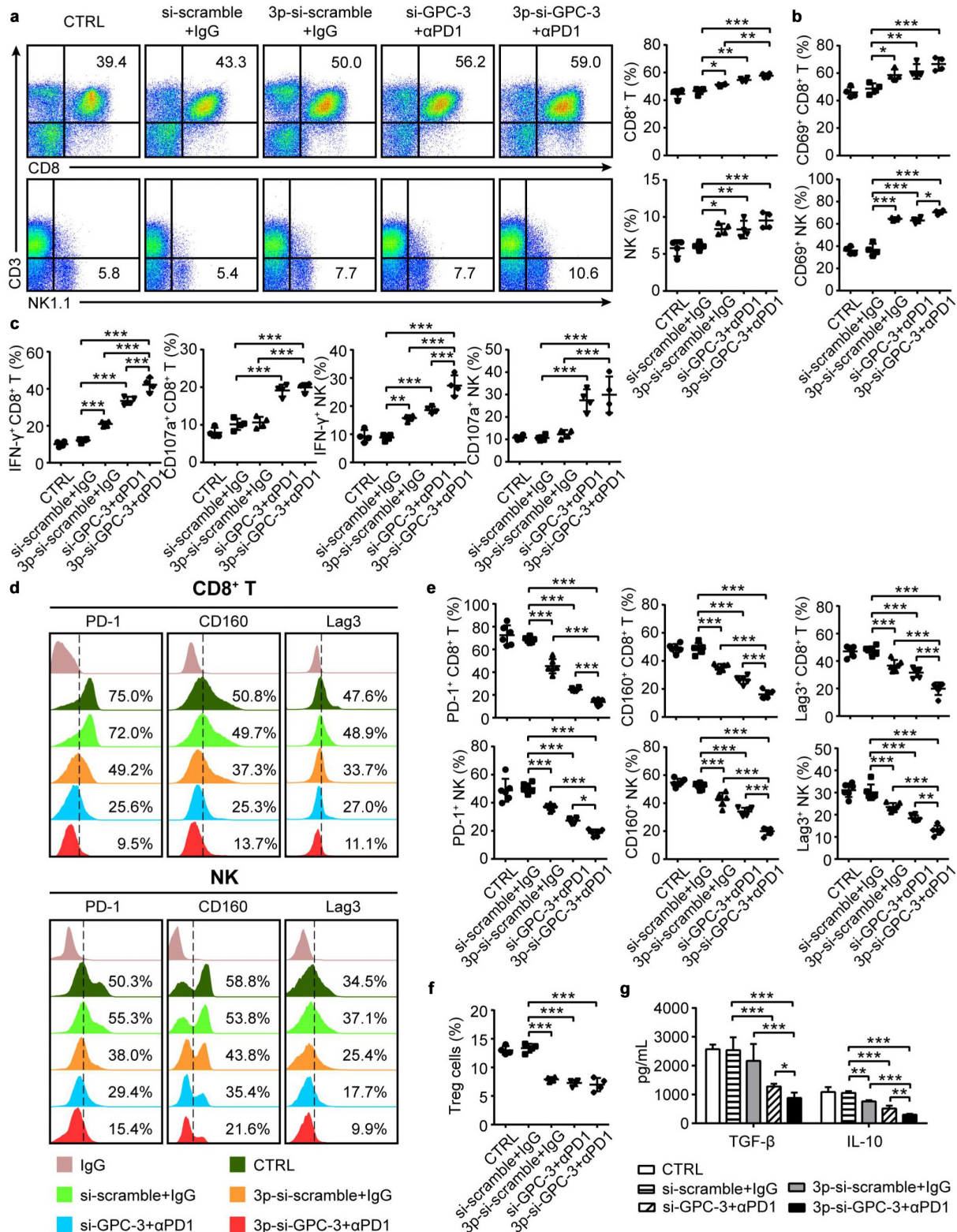


Figure 4. A combination of 3p-GPC-3 siRNA with anti-PD-1 antibody promotes immune responses in vivo. (a) The percentages of tumor-infiltrating CD8⁺ T cells and NK cells as determined by flow cytometry. (b) The percentages of tumor-infiltrating CD8⁺ T cells and NK cells expressing CD69, as determined by flow cytometry. (c) Flow cytometric analysis of the percentages of splenic CD8⁺ T cells and NK cells expressing IFN- γ and CD107a. (d) The percentages of tumor-infiltrating CD8⁺ T cells and NK cells expressing PD-1, CD160, or Lag3, as determined by flow cytometry. (e) Statistical analysis of the expression levels of inhibitory receptors in each treatment group in (d). (f) Flow cytometric analysis of the percentages of tumor-infiltrating Tregs. (g) Levels of TGF- β and IL-10 in the tumor homogenate, detected by ELISA. * $P < .05$, ** $P < .01$ or *** $P < .001$. $P > .05$ as no statistical difference (not shown).

in the CD8⁺ T cells and NK cells belonging to the anti-PD-1 and the combination treatment groups, while 3p-si-GPC-3 administration alone had no effect on CD107a expression (Figure 4c). These data indicate that PD-1 blockade can significantly enhance the CD8⁺ T cell- and NK cell-mediated anti-tumor effect of 3p-GPC-3 siRNA treatment.

Next, we wanted to know whether the state of immune exhaustion in the tumors of tumor-bearing mice could be reversed following PD-1 blockade. We examined some immune suppression indexes which were associated with the TME. Inhibitory molecules expression by CD8⁺ T cells and NK cells in the tumor tissues and spleens of tumor-bearing mice was initially determined by flow cytometry (the gating strategy is shown in Figure. S5). As shown in Figure 4d-e, the expression of inhibitory molecules PD-1, CD160, and Lag3 on tumor-infiltrating CD8⁺ T cells and NK cells was significantly decreased by treatment with 3p-si-GPC-3, an anti-PD-1 blocking antibody, and combination therapy, with combination treatment reducing the expression of these markers even further. Similarly, PD-1, CD160, and Lag3 expression on splenic CD8⁺ T cells and NK cells was lowest following combined 3p-si-GPC-3 and anti-PD-1 treatment (Fig. S6C-D). However, no significant changes in the expression of CTLA4, 2B4, and TIGIT by tumor-infiltrating and splenic CD8⁺ T cells and NK cells were observed (data not shown). In addition, we found that the proportions of tumor-infiltrating and splenic Tregs decreased as a result of anti-PD-1 treatment or combination (3p-si-GPC-3 and anti-PD-1) therapy, while there was no difference between the anti-PD-1 antibody group and the combination group (Figure 4f, Fig. S6E).

Finally, the levels of immunosuppressive cytokines TGF- β and IL-10 in the tumor homogenate and serum were assessed by ELISA. In the tumor homogenate, the level of TGF- β was significantly reduced after anti-PD-1 therapy and combination treatment but not following 3p-si-GPC-3 administration alone. The level of IL-10 was also reduced as a result of treatment with 3p-si-GPC-3 or anti-PD-1. In addition, the levels of TGF- β and IL-10 were lowest in the combination treatment group (Figure 4g). The circulating level of TGF- β in the serum was significantly inhibited by treatment with 3p-si-GPC-3 or PD-1 blockade, with the lowest TGF- β concentration seen in the combined treatment group. Moreover, serum IL-10 expression levels did not change after monotherapy or combination therapy (Fig. S6F).

Collectively, these results indicate that combination with PD-1 blockade enhances the anti-tumor effect of 3p-GPC-3 siRNA treatment by modulating the immune response, potentially by activating CD8⁺ T and NK cells and reversing immune exhaustion both locally and systemically.

Combining 3p-GPC-3 siRNA with PD-1 blockade elicits a potent anti-tumor immune memory response

The results reported above showed that PD-1 blockade could improve the anti-tumor effect of 3p-GPC-3 siRNA by eliciting anti-tumor immunity. Next, we explored whether the HCC-bearing mice had immune memory responses after 3p-GPC-3 siRNA and anti-PD-1 combination therapy. First, we tested

the ratio of central memory T cells (T_{CM}, CD3⁺CD8⁺CD44⁺CD62L⁺) and effector memory T cells (T_{EM}, CD3⁺CD8⁺CD44⁺CD62L⁻) in the tumor and spleen following treatment (the FACS gating strategy is shown in Figure. S7). We found that the frequencies of tumor-infiltrating T_{CM} and T_{EM} were increased in mice treated with 3p-si-GPC-3, anti-PD-1, and combination therapy. The highest frequency of T_{CM} was in combination therapy group and there was no difference between the anti-PD-1 and 3p-si-GPC-3 treatment groups (Figure 5a). The percentages of T_{EM} were higher in the anti-PD-1 treatment or combination therapy groups, compared with the 3p-si-GPC-3 treatment group, but there was no difference between the anti-PD-1 treatment and the combination therapy groups (Figure 5a). Furthermore, the percentages of splenic T_{CM} and T_{EM} were increased after anti-PD-1 treatment and combination therapy, however, 3p-si-GPC-3 treatment only improved the percentage of the T_{EM} subset. Of note, the highest frequencies of splenic T_{CM} and T_{EM} were observed in the combination therapy group (Fig. S8A).

Next, the expression of CD127 (a memory and differentiation marker) and KLRG1 (an effector marker)^{28,29} on the T_{CM} and T_{EM} subsets were determined. CD127 expression levels on tumor-infiltrating and splenic T_{CM} were increased following PD-1 blockade and combination therapy. 3p-si-GPC-3 therapy alone only increased CD127 expression on splenic T_{CM} but not tumor-infiltrating T_{CM}. The highest level of CD127 expression on tumor-infiltrating and splenic T_{CM} subset was observed in the combination therapy group (Figure 5b, Fig. S8B). The percentages of tumor-infiltrating and splenic T_{EM} expressing KLRG1 were also increased following PD-1 blockade and combination therapy. 3p-si-GPC-3 therapy increased the expression of KLRG1 on tumor-infiltrating but not splenic T_{EM}. Similarly, tumor-infiltrating and splenic T_{EM} in the combination therapy group were associated with the highest KLRG1 levels (Figure 5c, Fig. S8C). Nevertheless, there was no difference in the expression of KLRG1 on T_{CM} and CD127 on T_{EM} between the groups (Figure 5b-c, Fig. S8B-C). These results show that 3p-GPC-3 siRNA not only can improve the frequency of memory T cells but also maintain immune memory cells homeostasis by increasing the expression of CD127, and enhance the activation state of immune memory cells by increasing the expression of KLRG1. Moreover, combination with PD-1 blockade can further increase the proportions of immune memory cells and enhance the expression of CD127 and KLRG1 on T_{CM} or T_{EM} subsets. Together these results demonstrate that PD-1 blockade enhances the immune memory established following 3p-GPC-3 siRNA treatment.

Discussion

Immunotherapy for HCC is a rapidly evolving field, which in this past decade has transformed the oncology treatment landscape. A variety of strategies, such as cytokine administration, cancer vaccines, adoptive cellular therapy, and immune checkpoint blockade have been explored.³⁰⁻³² These strategies rely on the characteristics of the TME. Firstly, some proto-oncogenes promote tumor cell proliferation and inhibit

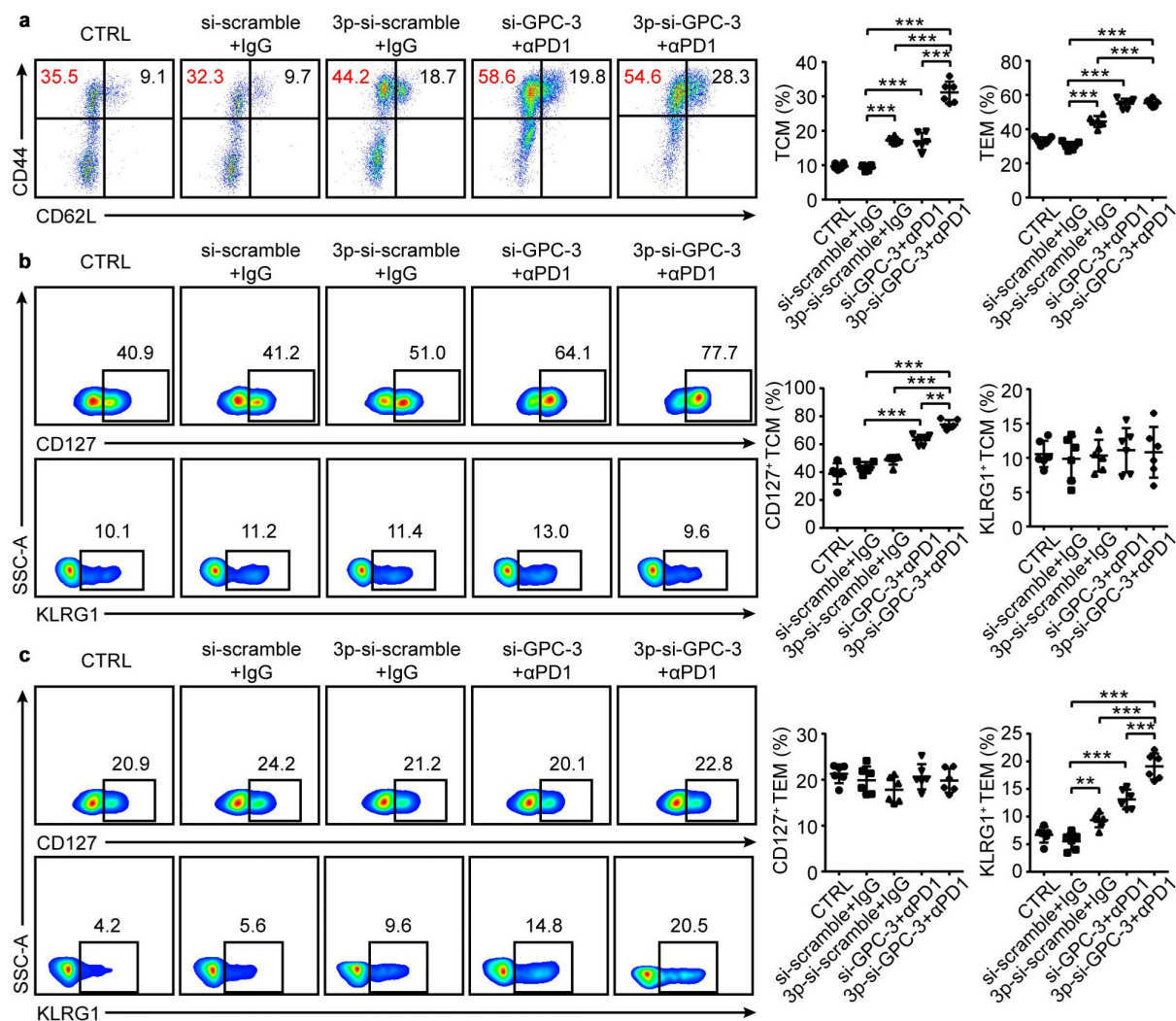


Figure 5. 3p-GPC-3 siRNA treatment combined with PD-1 blockade can increase the proportions of immune memory cells in the tumor. (a) The percentages of T_{CM} (CD44⁺CD62L⁺) and T_{EM} (CD44⁺CD62L⁻) cells (gated on CD3⁺CD8⁺) in the tumor were quantified following the different treatment regimens. The percentages of tumor-infiltrating T_{CM} expressing KLRG1 and CD127 (b) and T_{EM} expressing KLRG1 and CD127 (c) in the tumor-bearing mice were determined by flow cytometry. ***P* < .01 or ****P* < .001. *P* > .05 as no statistical difference (not shown).

tumor cell apoptosis, which are the main reasons for tumorigenesis.^{33,34} Secondly, immunosuppressive TMEs created by the presence of immunosuppressive cytokines, immunosuppressive cells (such as Tregs, MDSCs, and tumor stromal cells), and inhibitory molecules may cause immune cell dysfunction.^{35–39} Once dysfunctional, these immune cells are unable to recognize and eliminate liver cancer cells. Therefore, combination therapy designed to inhibit oncogene expression, stimulate anti-tumor immune responses, and reverse the immunosuppressive TME state, represents a novel promising treatment strategy.⁴⁰ In our study, we synthesized a short 5'-triphosphate (3p) RNA targeting GPC-3, 3p-GPC-3 siRNA, and showed that it exerted a therapeutic effect on HCC, which could be further improved when used in combination with PD-1 blockade.

Although GPC-3 is generally not detectable in the adult liver, it is abnormally expressed in HCC and contributes to its development.¹¹ We also found that GPC-3 is highly expressed in Hep1-6 cells (Fig. S1). To date, GPC-3 is being evaluated as a target for antibody-, gene-, and cell-based

therapies for HCC.^{41–43} These targeted therapies can specifically recognize the GPC-3 protein in cells and tissues, inhibit the proliferation of HCC cells, or induce apoptosis.^{44,45} To this end, we synthesized a small interfering RNA (siRNA) targeting GPC-3 that could inhibit the proliferation and induce apoptosis of Hep1-6 cells *in vivo* and *in vitro* (Figure 1).

In order to further determine the role of 3p-si-GPC-3 in promoting apoptosis, we assessed the protein levels of the apoptosis-associated molecules Bcl-2, Bcl-XL, Bax, and Caspase-3. Bcl-2 and its homologue Bcl-XL encode membrane-associated proteins that protect neoplastic cells from DNA damage-induced apoptosis, whereas Bax is a Bcl-2 antagonist that promotes cell death. Caspase-3 is a key executioner of the apoptosis pathway.⁴⁶ We found that 3p-si-GPC-3 noticeably reduced the levels of anti-apoptotic molecules Bcl-2 and Bcl-XL and increased those of the pro-apoptotic proteins Bax and Caspase-3 (Figure 1f).

In our previous studies, we established that 5'-triphosphate-siRNAs (3p-siRNAs) could activate the host RIG-I signaling pathway to successfully reverse hepatocyte-intrinsic immune-

tolerance.^{21,47} We also used a ssRNA-sh-Pim-3 dual-function vector to treat melanoma and found that type I IFNs could further enhance the activation and anti-tumor effect of CD8⁺ T and NK cells while reducing Tregs numbers.¹⁹ Increasing evidence has shown that 3p-siRNA is able to activate the RIG-I pathway and initiate the secretion of type I IFNs, which are heavily implicated in the regulation and activation of innate and adaptive immune responses.⁴⁸

In this study, we also found 3p-si-GPC-3 activated the RIG-I pathway and stimulated the secretion of IFN- α and IFN- β (Figure 1c, Fig. S1DE). In addition, our results showed that 3p-si-GPC-3 reversed the local anti-tumor immune responses at the tumor sites and restored systemic anti-tumor immunity, which was predominantly manifested in the activation of immune cells such as CD4⁺ T cells, CD8⁺ T cells, and NK cells (Figure 2a-b, Fig. S2A-B). The observed effect may be related to the activation of the immune system by type I IFNs. To determine which immune cells play an important role in halting tumor progression following 3p-si-GPC-3 treatment, we depleted of NK, CD4⁺ T, and CD8⁺ T cells. We found that both NK and CD8⁺ T cells were necessary for the anti-tumor effect exerted by 3p-si-GPC-3 (Figure 2d-e, Fig. S3B). Although CD8⁺ T and NK cells can infiltrate into HCC tumor sites to kill tumor cells, they may become dysfunctional due to the immunosuppressive TME, brought about by factors such as large numbers of infiltrating Tregs or MDSCs and high local TGF- β and IL-10 concentrations. These factors ultimately allow tumor escape and metastasis.⁴⁹ Our study showed that 3p-si-GPC-3 could subvert tumor-induced immunosuppression by reducing the percentages of Tregs and the levels of TGF- β and IL-10 in the TME (Figure 2c, Figure 4g).

It is well established that PD-L1 is highly expresses on HCC cells,⁵⁰ and that high PD-1 expression is a central feature of exhausted TILs.^{51,52} Therefore, immune checkpoint blockade has been the focus of cancer immunotherapy due to its promising outcomes across multiple advanced solid malignancies, including HCC.⁵³⁻⁵⁶ In this study, we confirmed that PD-L1 was highly expressed on Hepa1-6 cells and that PD-1 was abundant on tumor-infiltrating CD8⁺ T cells and NK cells, implying that blocking PD-1 may reverse CD8⁺ T cell and NK cell exhaustion (Fig. S4). With this in mind, we combined anti-PD-1 blockage with 3p-si-GPC-3 treatment. Consequently, we showed that blocking PD-1 could enhance the 3p-si-GPC-3-mediated anti-tumor effect (Figure 3).

We then assessed the effect of the blocking the PD-1/PD-L1 interaction on the immune system composition and function of tumor-bearing mice after 3p-si-GPC-3 treatment. We found that, compared with 3p-si-GPC-3 treatment alone, the combination therapy not only further increased the proportion of CD8⁺ T cells and NK cells while reducing Treg numbers but also increased the levels of activating cytokines while reducing the levels of inhibitory cytokines (Figure 4, Fig. S6). PD-1 blockade is known to induce T-box transcription factor (T-bet) expression in tumor-specific or self-reactive CD8⁺ T cells. Because T-bet represses a set of inhibitory receptors including PD-1, CD160, and Lag3,⁵⁷⁻⁵⁹ blocking PD-1 may also inhibit the expression of other immunosuppressive molecules. Notably, our results showed that combination therapy decreased PD-1 expression, which was accompanied by

a reduction in CD160 and Lag3 expression levels on tumor-infiltrating and splenic NK cells and CD8⁺ T cells (Figure 4d-e, Fig. S6C-D). These changes restored the function of intratumoral NK or CD8⁺ T cells, ultimately leading to the inhibition of tumor escape and growth.

The goal of cancer immunotherapy is to harness the host immune system to destroy tumor cells and elicit lasting immunity. Jacobson *et al*⁶⁰ reported that 3p-RNA could stimulate adaptive immunity to protect against tumor recurrence, when mice exhibiting complete responses were re-challenged with CT26 cells. Moreover, Ruzicka and colleagues⁶¹ found that 3p-RNA treatment induced immunological memory in preclinical AML models. Meanwhile, the RIG-I agonist, SLR14, inhibited B16 tumor growth, curing mice that had developed an immune memory.⁶² These studies indicate that 3p-RNA may induce immune memory by activating the RIG-I pathway. Our results support these findings. In the present study, the tumor-bearing mice developed immune memory to Hepa1-6 cells after 3p-si-GPC-3 treatment (Figure 5). On determining the ratio of T_{CM} and T_{EM} in the tumor and spleen after treatment, we found that 3p-si-GPC-3 administration improved the percentages of tumor-infiltrating and splenic T_{EM}, but only splenic T_{CM}. This may be related to the type I IFNs secreted as a consequence of RIG-I pathway activation. Vahed *et al*⁶³ found that T_{EM} expressed high levels of type I IFNs, however, this mechanism needs to be further investigated. In the acute phase of immune recognition, CD8⁺ effector T cells are destined to become CD127-expressing memory T cells that share multiple features with conventional memory CD8⁺ T cells (e.g., superior proliferative capacity and long-term survival in the absence of antigen).^{64,65} Interestingly, the establishment of CD127⁺ memory T cells also depends on a prolonged duration of the initial antigen exposure.⁶⁶ KLRG1 is an important active antigen-specific T cell marker.⁶⁷ Our results showed that the expression of CD127 on T_{CM} and KLRG1 on T_{EM} were significantly increased after 3p-si-GPC-3 therapy. These data indicate that 3p-GPC-3 siRNA treatment not only improves the polyfunctionality of tumor-specific T cells but also the proliferation and killing capacity of immune memory cells. Kurtulus and colleagues⁶⁸ found that PD-1⁻ CD8⁺ TILs comprised tumor-antigen-specific precursors that expanded in response to checkpoint and PD-1 blockade, and could induce memory- and effector-like transcriptional programs in murine and human samples. In line with this work, we demonstrated that combination treatment was more beneficial for forming immune memory than anti-PD-1 or 3p-si-GPC-3 treatment alone. PD-1 blockade appears to provide additional help for boosting CD8⁺ T cell-mediated immunity and possibly eliciting a potent T cell-mediated memory response to tumor re-challenge, as shown in our study (Figure 5, Fig. S8).

In summary, we have studied the therapeutic effect of 3p-GPC-3 siRNA on HCC for the first time and demonstrated that PD-1 blockade improves the therapeutic effect observed following 3p-GPC-3 siRNA administration alone. While 3p-GPC-3 siRNA directly activates the innate immune response, PD-1 blockade directly activates the adaptive immune response. Thus, combining 3p-GPC-3 siRNA with anti-PD-1 treatment

effectively activates both arms of the immune system, serving to reverse immune exhaustion and elicit a potent anti-tumor memory response both locally and systemically. Our work has shown that combining 3p-GPC-3 siRNA with anti-PD-1 elicits a powerful therapeutic effect against HCC. This strategy may therefore represent a promising approach for the treatment of HCC and other solid tumors, in which GPC-3 is aberrantly expressed.

Acknowledgments

We thank Translational Medicine Core Facility of Shandong University for consultation and instrument availability that supported this work.

Author Contributions

Liwei Shao and Xin Yu designed and performed experiments, analyzed data, and wrote the manuscript. Xinke Zhang provided professional technical support for *in vivo* imaging and analysis. Qiuju Han and Nan Lu provided guidance for the experiment design and contributed to analyzing and discussing the data. Cai Zhang conceived and supervised the study, designed experiments, analyzed and interpreted data, and wrote the manuscript. All authors read and approved the final manuscript.

Disclosure statement

There don't have potential conflicts of interest between the authors.

Funding

The National Natural Science Foundation of China (91842305, 81771686), the Shandong Provincial Key Research and Development Program (Major Scientific and Technological Innovation Project) (Shandong Provincial Key Research and Development Program (Major Scientific and Technological Innovation Project) 2019JZZY021013), and the Shandong Provincial Natural Science Foundation (ZR2020MH260).

ORCID

Cai Zhang  <http://orcid.org/0000-0002-3849-6676>

References

- Sung H, Ferlay J, Siegel RL, Mathieu L, Isabelle S, Jemal A, Bray F. Global cancer statistics 2020: GLOBOCAN estimates of incidence and mortality worldwide for 36 cancers in 185 countries. *CA: A Cancer Journal for Clinicians*. 2021;71(3):209–249. doi:10.3322/caac.21660.
- Llovet JM, Kelley RK, Villanueva A, Singal AG, Pikarsky E, Roayaie S, Lencioni R, Koike K, Zucman-Rossi J, Finn RS. Hepatocellular carcinoma. *Nature Reviews. Disease Primers*. 2021;7(1):6–34. doi:10.1038/s41572-020-00240-3.
- Pfister D, Núñez NG, Pinyol R, Govaere O, Pinter M, Szydlowska M, Gupta R, Qiu M, Deczkowska A, Weiner A, et al. NASH limits anti-tumour surveillance in immunotherapy-treated HCC. *Nature*. 2021;592(7854):450–456. doi:10.1038/s41586-021-03362-0.
- Jiang X, Wang J, Deng X, Xiong F, Ge JS, Xiang B, Wu X, Ma J, Zhou M, Li XL, et al. Role of the tumor microenvironment in PD-L1/PD-1-mediated tumor immune escape. *Molecular Cancer*. 2019;18(1):10–27. doi:10.1186/s12943-018-0928-4.
- Zhao YJ, Shao QX, Peng GY. Exhaustion and senescence: two crucial dysfunctional states of T cells in the tumor microenvironment. *Cellular & Molecular Immunology*. 2020;17(1):27–35. doi:10.1038/s41423-019-0344-8.
- Zhang XQ, Cheng C, Hou JY, Qi XY, Wang X, Han P, Yang XM. Distinct contribution of PD-L1 suppression by spatial expression of PD-L1 on tumor and non-tumor cells. *Cellular & Molecular Immunology*. 2019;16(4):392–400. doi:10.1038/s41423-018-0021-3.
- Huang X, Zhang XZ, Bai XL, Liang TB. Blocking PD-L1 for anti-liver cancer immunity: USP22 represents a critical cotarget. *Cellular & Molecular Immunology*. 2020;17(7):677–679. doi:10.1038/s41423-019-0348-4.
- El-Khoueiry AB, Sangro B, Yau T, Crocenzi TS, Kudo M, Hsu C, Kim TY, Choo SP, Trojan J, Welling TH, et al. Nivolumab in patients with advanced hepatocellular carcinoma (Check Mate 040): an open-label, non-comparative, phase 1/2 dose escalation and expansion trial. *The Lancet*. 2017;389(10088):2492–2502. doi:10.1016/S0140-6736(17)31046-2.
- Capurro M, Izumikawa T, Suarez P, Shi W, Cydzik M, Kaneiwa T, Gariepy J, Bonafe L, Filmus J. Glypican-6 promotes the growth of developing long bones by stimulating Hedgehog signaling. *The Journal of Cell Biology*. 2017;216(9):2911–2926. doi:10.1083/jcb.201605119.
- Li N, Gao W, Zhang YF, Ho M. Glypicans as cancer therapeutic targets. *Trends in Cancer*. 2018;4(11):741–754. doi:10.1016/j.trecan.2018.09.004.
- Zhou F, Shang W, Yu X, Tian J. Glypican-3: a promising biomarker for hepatocellular carcinoma diagnosis and treatment. *Medicinal Research Reviews*. 2018;38(2):741–767. doi:10.1002/med.21455.
- Li N, Wei L, Liu X, Bai HJ, Ye Y, Li D, Li N, Baxa U, Wang Q, Lv L, et al. A frizzled-like cysteine-rich domain in Glypican-3 mediates Wnt binding and regulates hepatocellular carcinoma tumor growth in mice. *Hepatology*. 2019;70(4):1231–1245. doi:10.1002/hep.30646.
- Setten RL, Rossi JJ, Han SP. The current state and future directions of RNAi-based therapeutics. *Nature Reviews Drug Discovery*. 2019;18(6):421–446. doi:10.1038/s41573-019-0017-4.
- Meng Z, Lu M. RNA interference-induced innate immunity, off-target effect, or immune adjuvant? *Frontiers in Immunology*. 2017;8:331. doi:10.3389/fimmu.2017.00331.
- Choi JH, Burke JM, Szymanik KH, Nepal U, Battenhouse A, Lau JT, Stark A, Lam V, Sullivan CS. DUSP11-mediated control of 5'-triphosphate RNA regulates RIG-I sensitivity. *Genes & Development*. 2020;34(23–24):1697–1712. doi:10.1101/gad.340604.120.
- Singh N, Ranjan P, Cao W, Patel J, Gangappa S, Davidson BA, Sullivan JM, Prasad PN, Knight PR, Sambhara S. A dual-functioning 5'-PPP-NS1shRNA that activates a RIG-I antiviral pathway and suppresses influenza NS1. *Molecular Therapy Nucleic Acids*. 2020;19:1413–1422. doi:10.1016/j.omtn.2020.01.025.
- Jiang M, Zhang S, Yang Z, Lin HY, Zhu J, Liu L, Wang WD, Liu S, Liu W, Ma YW, et al. Self-recognition of an inducible host lncRNA by RIG-I feedback restricts innate immune response. *Cell*. 2018;173(4):906–919. doi:10.1016/j.cell.2018.03.064.
- Ou DL, Chen CW, Hsu CL, Chung CH, Feng ZR, Le BS, Cheng AL, Yang MH, Hsu C. Regorafenib enhances antitumor immunity via inhibition of p38 kinase/Creb1/Klf4 axis in tumor-associated macrophages. *J Immunother Cancer*. 2021;9(3):e001657. doi:10.1136/jitc-2020-001657.
- Liu J, Hu Y, Guo Q, Yu X, Shao LW, Zhang C. Enhanced anti-melanoma efficacy of a Pim-3-targeting bifunctional small hairpin RNA via single-stranded RNA-mediated activation of plasmacytoid dendritic cells. *Frontiers in Immunology*. 2019;10:2721–2735. doi:10.3389/fimmu.2019.02721.
- Guo Q, Lan P, Yu X, Han QJ, Zhang J, Tian ZG, Zhang C. Immunotherapy for hepatoma using a dual-function vector with both immunostimulatory and pim-3-silencing effects. *Molecular Cancer Therapeutics*. 2014;13(6):1503–1513. doi:10.1158/1535-7163.MCT-13-0722.
- Han Q, Zhang C, Zhang J, Tian ZG. Reversal of hepatitis B virus-induced immune tolerance by an immunostimulatory 3p-HBx-siRNAs in a retinoic acid inducible gene I-dependent manner. *Hepatology*. 2011;54(4):1179–1189. doi:10.1002/hep.24505.

22. Dong ZZ, Yao M, Wang L, Yang JL, Yao DF. Down-regulating Glypican-3 expression: molecular-targeted therapy for hepatocellular carcinoma. *Mini-Reviews in Medicinal Chemistry*. 2014;14(14):1183–1193. doi:10.2174/1389557515666150101105135.
23. Borden EC. Interferons alpha and beta in cancer: therapeutic opportunities from new insights. *Nature Reviews Drug Discovery*. 2019;18(3):219–234. doi:10.1038/s41573-018-0011-2.
24. Wedekind A, Fritzs D, Kröger A. Add on the next level—the time point of the type I IFN response orchestrates the immune response. *Cellular & Molecular Immunology*. 2020;17(8):791–793. doi:10.1038/s41423-020-0442-7.
25. Yarchoan M, Xing D, Luan L, Xu HY, Sharma RB, Popovic A, Pawlik TM, Kim AK, Zhu QF, Jaffee EM, et al. Characterization of the immune microenvironment in Hepatocellular Carcinoma. *Clinical Cancer Research*. 2017;23(23):7333–7339. doi:10.1158/1078-0432.CCR-17-0950.
26. Liu Y, Cheng Y, Xu Y, Wang Z, Du X, Li C, Peng J, Gao L, Liang X, Ma C. Increased expression of programmed cell death protein 1 on NK cells inhibits NK-cell-mediated anti-tumor function and indicates poor prognosis in digestive cancers. *Oncogene*. 2017;36(44):6143–6153. doi:10.1038/onc.2017.209.
27. Sun C, Lan P, Han Q, Huang M, Zhang ZH, Xu GL, Song JX, Wang JY, Wei HM, Zhang J, et al. Oncofetal gene SALL4 reactivation by hepatitis B virus counteracts miR-200c in PD-L1-induced T cell exhaustion. *Nature Communications*. 2018;9(1):1241–1258. doi:10.1038/s41467-018-03584-3.
28. Kaech SM, Tan JT, John Wherry E, Konieczny BT, Surh CD, Ahmed R. Selective expression of the interleukin 7 receptor identifies effector CD8 T cells that give rise to long-lived memory cells. *Nature Immunology*. 2003;4(12):1191–1198. doi:10.1038/ni1009.
29. Aki Hoji ID, Popescu MR, Pipeling PD, Shah SA, Winters JF, McDyer. Early KLRG1⁺ but not CD57⁺CD8⁺ T cells in primary CMV infection predict effector function and viral control. *J Immunol*. 2019;203(8):2063–2075. doi:10.4049/jimmunol.1900399.
30. Zhang H, Chen J. Current status and future directions of cancer immunotherapy. *Journal of Cancer*. 2018;9(10):1773–1781. doi:10.1038/s41571-018-0073-4.
31. Ruf B, Heinrich B, Greten TF. Immunobiology and immunotherapy of HCC: spotlight on innate and innate-like immune cells. *Cellular & Molecular Immunology*. 2021;18:112–127. doi:10.1038/s41423-020-00572-w.
32. Feng D, Gao B. From basic liver immunology to therapeutic opportunities for liver diseases. *Cellular & Molecular Immunology*. 2021;18(1):1–3. doi:10.1038/s41423-020-00607-2.
33. Zucman-Rossi J, Villanueva A, Nault J-C, Llovet JM. Genetic landscape and biomarkers of hepatocellular carcinoma. *Gastroenterology*. 2015;149(5):1226–1239. doi:10.1053/j.gastro.2015.05.061.
34. Casey SC, Baylot V, Felsher DW. MYC: master regulator of immune privilege. *Trends in Immunology*. 2017;38(4):298–305. doi:10.1016/j.it.2017.01.002.
35. Binnewies M, Roberts EW, Kersten K, Chan V, Fearon DF, Merad M, Coussens LM, Gabrilovich DI, Ostrand-Rosenberg S, Hedrick CC, et al. Understanding the tumor immune microenvironment (TIME) for effective therapy. *Nature Medicine*. 2018;24(5):541–550. doi:10.1038/s41591-018-0014-x.
36. Zhou SL, Zhou ZJ, Hu ZQ, Huang XW, Wang Z, Chen EB, Fan J, Cao Y, Dai Z, Zhou J. Tumor-associated neutrophils recruit macrophages and T-regulatory cells to promote progression of hepatocellular carcinoma and resistance to sorafenib. *Gastroenterology*. 2016;150(7):1646–1658. doi:10.1053/j.gastro.2016.02.040.
37. Cheng H, Ma K, Zhang L, Li G. The tumor microenvironment shapes the molecular characteristics of exhausted CD8⁺ T cells. *Cancer Letters*. 2021;506:55–66. doi:10.1016/j.canlet.2021.02.013.
38. Habif G, Crinier A, André P, Vivier E, Narni-Mancinelli E. Targeting natural killer cells in solid tumors. *Cellular & Molecular Immunology*. 2019;16(5):415–422. doi:10.1038/s41423-019-0224-2.
39. Pan X, Zheng L. Epigenetics in modulating immune functions of stromal and immune cells in the tumor microenvironment. *Cellular & Molecular Immunology*. 2020;17(9):940–953. doi:10.1038/s41423-020-0505-9.
40. Varadé J, González-Fernández MS. Á. Human immunology and immunotherapy: main achievements and challenges. *Cellular & Molecular Immunology*. 2021;18:805–828. doi:10.1038/s41423-020-00530-6.
41. Fu Y, Urban DJ, Nani RR, Zhang YF, Li N, Fu HY, Shah H, Gorka AP, Guha R, Chen L, et al. Glypican-3-specific antibody drug conjugates targeting hepatocellular carcinoma. *Hepatology*. 2019;70(2):563–576. doi:10.1002/hep.30326.
42. Wu X, Luo H, Shi B, Di SM, Sun RX, Su JW, Ying L, Li H, Jiang H, Li ZH. Combined antitumor effects of sorafenib and GPC3-CAR T Cells in mouse models of hepatocellular carcinoma. *Molecular Therapy: The Journal of the American Society of Gene Therapy*. 2019;27(8):1483–1494. doi:10.1016/j.ymthe.2019.04.020.
43. Nishida T, Kataoka H. Glypican 3-targeted therapy in hepatocellular carcinoma. *Cancers*. 2019;11(9):1339–1352. doi:10.3390/cancers11091339.
44. Wu Q, Pi L, Le Trinh T, Zuo CH, Xia M, Jiao Y, Hou ZH, Jo S, Puszyk W, Pham K, et al. A novel vaccine targeting Glypican-3 as a treatment for hepatocellular carcinoma. *Molecular Therapy: The Journal of the American Society of Gene Therapy*. 2017;25(10):2299–2308. doi:10.1016/j.ymthe.2017.08.005.
45. Zhu AX, Gold PJ, El-Khoueiry AB, Abrams TA, Morikawa H, Ohishi N, Ohtomo T, Philip PA. First-in-man phase I study of GC33, a novel recombinant humanized antibody against glypican-3, in patients with advanced hepatocellular carcinoma. *Clinical Cancer Research: An Official Journal of the American Association for Cancer Research*. 2013;19(4):920–928. doi:10.1158/1078-0432.CCR-12-2616.
46. Wallach D, Kang TB. Programmed cell death in immune defense: knowledge and presumptions. *Immunity*. 2018;49(1):19–32. doi:10.1016/j.immuni.2018.06.019.
47. Lan P, Zhang C, Han Q, Zhang J, Tian ZG. Therapeutic recovery of hepatitis B virus (HBV)-induced hepatocyte-intrinsic immune defect reverses systemic adaptive immune tolerance. *Hepatology*. 2013;58(1):73–85. doi:10.1002/hep.26339.
48. Lee J, Park EB, Min J, Sung SE, Jang YY, Shin JS, Chun DM, Kim KH, Hwang J, Lee MK, et al. Systematic editing of synthetic RIG-I ligands to produce effective antiviral and anti-tumor RNA immunotherapies. *Nucleic Acids Res*. 2018;46(4):1635–1647. doi:10.1093/nar/gky819.
49. Ringelhan M, Pfister D, O’connor T, Pikarsky E, Heikenwalder M. The immunology of hepatocellular carcinoma. *Nature Immunology*. 2018;19(3):222–232. doi:10.1038/s41590-018-0044-z.
50. Li H, Li CW, Li X, Guo L, Liu S, Liu CX, Lai CC, Hsu JM, Dong QZ, Xia WY, et al. MET inhibitors promote liver tumor evasion of the immune response by stabilizing PDL1. *Gastroenterology*. 2019;156(6):1849–1861. doi:10.1053/j.gastro.2019.01.252.
51. Li H, Li X, Liu S, Guo L, Zhang B, Zhang JB, Ye QH. Programmed cell death-1 (PD-1) checkpoint blockade in combination with a mammalian target of rapamycin inhibitor restrains hepatocellular carcinoma growth induced by hepatoma cell-intrinsic PD-1. *Hepatology*. 2017;66(6):1920–1933. doi:10.1002/hep.29360.
52. Sharpe AH, Pauken KE. The diverse functions of the PD1 inhibitory pathway. *Nature Reviews Immunology*. 2018;18(3):153–167. doi:10.1038/nri.2017.108.
53. Pinter M, Jain RK, Duda DG. The current landscape of immune checkpoint blockade in hepatocellular carcinoma: a review. *JAMA Oncol*. 2021;7(1):113–123. doi:10.1001/jamaoncol.2020.3381.
54. Zhang C, Liu YX. Targeting NK cell checkpoint receptors or molecules for cancer immunotherapy. *Front. Immunol*. 2020;11:1295. doi:10.3389/fimmu.2020.01295.
55. Sivori S, Vacca P, Del Zotto G, Munari E, Mingari MC, Human ML. NK cells: surface receptors, inhibitory checkpoints, and translational applications. *Cellular & Molecular Immunology*. 2019;16(5):430–441. doi:10.1038/s41423-019-0206-4.

56. Ben-Shmuel A, Biber G, Sabag B, Barda-Saad M. Modulation of the intracellular inhibitory checkpoint SHP-1 enhances the antitumor activity of engineered NK cells. *Cellular & Molecular Immunology*. 2021;18(5):1314–1316. doi:10.1038/s41423-020-0443-6.
57. Berrien-Elliott MM, Yuan J, Swier LE, Jackson SR, Chen CL, Donlin MJ, Teague RM. Checkpoint blockade immunotherapy relies on T-bet but not Eomes to induce effector function in tumor-infiltrating CD8⁺ T Cells. *Cancer Immunology Research*. 2015;3(2):116–124. doi:10.1158/2326-6066.CIR-14-0159.
58. Kao C, Oestreich KJ, Paley MA, Crawford A, Angelosanto JM, Ali MA, Intlekofer AM, Boss JM, Reiner SL, Weinmann AS. Transcription factor T-bet represses expression of the inhibitory receptor PD-1 and sustains virus-specific CD8⁺ T cell responses during chronic infection. *Nature Immunology*. 2011;12(7):663–671. doi:10.1038/ni.2046.
59. Beltra JC, Manne S, Abdel-Hakeem MS, Kurachi M, Giles JR, Chen Z, Casella V, Ngiow SF, Khan O, Huang YJ, et al. Developmental relationships of four exhausted CD8⁺ T Cell subsets reveals underlying transcriptional and epigenetic landscape control mechanisms. *Immunity*. 2020;52(5):825–841. doi:10.1016/j.immuni.2020.04.014.
60. Jacobson ME, Wang-Bishop L, Becker KW, Wilson JT. Delivery of 5'-triphosphate RNA with endosomolytic nanoparticles potentially activates RIG-I to improve cancer immunotherapy. *Biomaterials Science*. 2019;7(2):547–559. doi:10.1039/c8bm01064a.
61. Ruzicka M, Koenig LM, Formisano S, Boehmer DR, Vick B, Heuer EM, Mein H, Kocheise L, Zeithöfler M, Ahlfeld J. RIG-I-based immunotherapy enhances survival in preclinical AML models and sensitizes AML cells to checkpoint blockade. *Leukemia*. 2019;34(4):1017–1026. doi:10.1038/s41375-019-0639-x.
62. Jiang X, Muthusamy V, Fedorova O, Kong Y, Kim DJ, Bosenberg M, Pyle AM, Iwasaki A. Intratumoral delivery of RIG-I agonist SLR14 induces robust antitumor responses. *Journal of Experimental Medicine*. 2019;216(12):2854–2868. doi:10.1084/jem.20190801.
63. Vahed H, Agrawal A, Srivastava R, Prakash S, Coulon P-G A, Roy S, Mohamed LB. Unique type I interferon, expansion/survival cytokines, and JAK/STAT gene signatures of multi-functional herpes simplex virus-specific effector memory CD8⁺ TEM cells are associated with asymptomatic herpes in humans. *Journal of Virology*. 2019;93(4):e01882–18. doi:10.1128/JVI.01882-18.
64. Shin MS, You S, Kang Y, Lee N, Yoo SA, Park K, Kang KS, Kim SH, Mohanty S, Shawet AC, et al. DNA methylation regulates the differential expression of CX3CR1 on human IL-7Rα^{low} and IL-7Rα^{high} effector memory CD8⁺ T Cells with distinct migratory capacities to the fractalkine. *Journal of Immunology*. 2015;195(6):2861–2869. doi:10.4049/jimmunol.1500877.
65. Park HJ, Shin MS, Kim M, Bilsborrow JB, Mohanty S, Montgomery RR, Shaw AC, You S, Insoo K. Transcriptomic analysis of human IL-7 receptor alpha^{low} and alpha^{high} effector memory CD8⁺ T cells reveals an age-associated signature linked to influenza vaccine response in older adults. *Aging Cell*. 2019;18(4):e12960. doi:10.1111/ace1.12960.
66. Bachmann MF, Beerli RR, Agnellini P, Schwarz K, Oxenius A, Oxenius A. Long-lived memory CD8⁺ T cells are programmed by prolonged antigen exposure and low levels of cellular activation. *European Journal of Immunology*. 2006;36(4):842–854. doi:10.1002/eji.200535730.
67. Herndler-Brandstetter D, Ishigame H, Shinnakasu R, Plajer V, Stecher C, Jun Z, Lietzenmayer M, Kroehling L, Takumi A, Kometani K, et al. KLRG1⁺ effector CD8⁺ T Cells lose KLRG1, differentiate into all memory T cell lineages, and convey enhanced protective immunity. *Immunity*. 2018;48(4):716–729. doi:10.1016/j.immuni.2018.03.015.
68. Kurtulus S, Madi A, Escobar G, Klapholz M, Nyman J, Christian E, Pawlak M, Dionne D, Xia JR, Rozenblatt-Rosen O, et al. Checkpoint blockade immunotherapy induces dynamic changes in PD-1^{hi}CD8⁺ tumor-infiltrating T Cells. *Immunity*. 2019;50(1):181–194. doi:10.1016/j.immuni.2018.11.014.